Talanta 99 (2012) 180–185

Contents lists available at SciVerse ScienceDirect

Talanta

journal homepage: www.elsevier.com/locate/talanta

Portable mercury sensor for tap water using surface plasmon resonance of immobilized gold nanorods

Emily C. Heider, Khang Trieu, Anthony F.T. Moore, Andres D. Campiglia *

Department of Chemistry, University of Central Florida, P.O. Box 25000, Orlando, Florida 32816-2366, USA

ARTICLE INFO

Article history:
Received 13 March 2012
Received in revised form
16 May 2012
Accepted 18 May 2012
Available online 26 May 2012

Keywords:
Localized surface plasmon resonance
Gold nanoparticles
Mercury detection
Sensors

ABSTRACT

The surface plasmon resonance of surface immobilized gold nanorods (Au NRs) was used to quantify mercury in tap water. Glass substrates were chemically functionalized with (3-mercaptopropyl) trimethoxysilane, which chemically bound the nanorods to produce a portable and sensitive mercury sensor. The analytical capabilities of the sensor were measured using micromolar mercury concentrations. Since the analytical response was dependent upon number of nanorods present, the limit of detection was 2.28×10^{-19} M mercury per nanorod. The possibility to using glass substrates with immobilized Au NRs is a significant step towards the analysis of mercury in tap water flows at this low concentration level.

1. Introduction

The utility of noble metal nanorods (NR) in sensing devices has been demonstrated in a variety applications, including the monitoring of biomolecular binding, [1,2] elucidation of molecular motion, [3,4] and enhancement of fluorescence [5,6] and Raman scattering [7]. The design of these nano-scale sensors frequently exploit the localized surface plasmon resonance (LSPR) that arises from the resonant oscillation of electrons, which is sensitive to the refractive index of the surrounding medium, the composition of the NR, as well as their dimensions (see Mayer et al. for a recent review) [8]. Recent work in developing myriad facile NR immobilization strategies [9–12] and characterizing [2,3,13] the resulting surfaces has advanced the possibility of utilizing immobilized NR sensors in routine analysis.

Herein, we describe an application of a well-studied immobilization strategy to create gold (Au) NR-based sensors that are sensitive to quantity, and selective for the presence of mercury. A known environmental pollutant, mercury can damage brain, heart, kidney and lungs; portable and robust methods for detecting mercury may have important utility. While several means for accurate and sensitive quantification of mercury exist, including atomic absorbance [14] and fluorescence spectroscopy, [15] voltammetric electrochemical methods, [16] and peizo-electric quartz crystals, [17] a platform for practical, portable on-site analysis could prove useful.

Previously, the sensitivity of Au NR to metallic mercury was demonstrated by Rex et al. [18] wherein the dual SPR peaks, related to the axial and longitudinal dimensions of the NR, indicated the concentration of mercury due to the Au-mercury interaction. In that case, the known affinity for Au and metallic mercury causes in amalgam formation, resulting an alterations to the structure of the NR that can be monitored by recording the absorption spectra of colloidal NRs. That work is extended here with the use of silica substrates that are chemically functionalized with (3-mercaptopropyl)trimethoxysilane (MPTMS). The thiol group on the MPTMS provides a capture surface for the Au NRs. The shifting of the LSPR peak maximum in the absorption spectra was observed when the longitudinal:axial aspect ratio changed linearly with respect to the mercury concentration in the presence of the NRs. The analytical figures of merit (AFOM) for the detection and quantification of mercury using the sensors are described, including characterization of the sensing substrate.

2. Experimental

2.1. Chemicals and reagents

All experiments used analytical-reagent grade chemicals. Hydrogen peroxide (30%), hexadecyltrimethylammonium bromide (CTAB) and (3-mercaptopropyl)trimethoxysilane (MPTMS) were purchased at Sigma-Aldrich. Au NR with peak LSPR wavelengths 615 nm (6.29×10^{11} nanorods/mL), and 750 nm (5.77×10^{10} nanorods/mL) were purchased from Nanopartz, Inc. (Loveland, CO). According to the manufacturer, their average dimensions were 25×51 nm and

* Corresponding author. Tel.: +1 407 823 4162; fax: +1 407 823 2252.
E-mail addresses: Emily.Heider@ucf.edu (E.C. Heider), khangtrieu818@knights.ucf.edu (K. Trieu), aftmoore@gmail.com (A.F.T. Moore), Andres.campiglia@ucf.edu (A.D. Campiglia).

0039-9140/$ - see front matter © 2012 Elsevier B.V. All rights reserved.
http://dx.doi.org/10.1016/j.talanta.2012.05.037

25×71 nm. Ethanol, sodium borohydride, mercury (II) chloride, sodium nitrate, lead (II) nitrate, copper sulfate, arsenic pentoxide, and sodium chloride were purchased from Fisher Scientific. Water (18 MΩ cm) was purified using a Barnstead Infinity Filter.

2.2. Instrumentation

A Cary 50 (Varian) single beam spectrometer was used to record absorbance measurements. The illumination source was a 75-Watt pulsed xenon lamp with 2-nm fixed band-pass. Instrumental performance was monitored with a commercial standard (Photon Technology International) consisting of a single crystal of dysprosium-activated yttrium aluminum garnet mounted in a cuvette-sized holder with a well-characterized quasi-line absorption spectrum. Wavelength accuracy was evaluated periodically by comparing the recorded position of several spectral lines to the maximum wavelengths provided by the manufacturer. The standard deviations of the average maximum wavelengths obtained from repetitive scans within 300–800 nm confirmed the performance of the spectrometer according to specifications (± 0.02 nm). When testing solutions, a 600 μL quartz cuvette was used with 1-cm path length. To examine the absorbance of the Au NR-modified substrates, the substrates were placed against the face of a 1 cm quartz cuvette in the optical path.

Bright field images were acquired using a Nikon TE-2000U microscope equipped with a mercury lamp and 0.52 numerical aperture (NA) condenser. A Plan-Fluor 60X air objective (0.70 NA) collected the light that was imaged using a Rettiga 1300i Fast 1394 CCD detector and QImaging software.

A Zeiss-ULTRA-55 FEG SEM was used to acquire images with an in-lens detector. An electron acceleration voltage of 2 kV was used to minimize charging the sample surface. Prior to imaging, surfaces were coated with a graphite layer using vacuum deposition.

2.3. Gold nanoparticle immobilization

Glass cover slides were functionalized using the procedure detailed by Okamoto and Yamaguchi [10]. The cover slides were first cleaned using piranha solution (30% H_2O_2 mixed in a 1:4 ratio with concentrated H_2SO_4) for twenty minutes and rinsed with copious amounts of water. The slides were dried and then immersed in a solution containing 10% ethanol and 90% MPTMS (volume percent) for 10 min. The slides were again rinsed with copious quantities of methanol before being immersed in the colloidal Au nanoparticle solutions for two hours. Prior to immobilization, the Au NR solutions were chemically reduced using 0.100 M sodium borohydride as a reducing agent. The concentrations of the nanoparticle solutions varied based on the solution provided by the supplier, for the nanoparticles with 615 nm LSPR maximum, the concentration was 2.2×10^{11} nanoparticles/mL. The slides were left in solution for 2 h; longer times resulted in aggregation of NRs on the surface of the substrate.

2.4. Mercury detection measurements

Chemically functionalized glass cover-slides with immobilized Au NRs on the surface were immersed in water and placed in a cuvette in the beam path of a UV–vis spectrophotometer. Since the amalgam formation between mercury and Au forms only with metallic Hg (0), 2.22×10^{-4} M $HgCl_2$ was chemically reduced using 0.100 M sodium borohydride. The mercury was reduced prior to addition to the cuvette containing the Au NR sensor. Small volumes of mercury were added to the cuvette and allowed to react (10 min for immobilized NRs and 4 min for NRs in solution) and the absorbance spectra were measured after the additions, yielding a range of Hg concentrations from 1.0–50.0 μM.

3. Results and discussion

3.1. Imaging immobilized NRs

Substrates with immobilized Au NRs were prepared according to Okamoto and Yamaguchi [10]. Images of the surface were acquired using scanning electron microscopy. Similar to the example shown in Fig. 1, a low incidence of NRs aggregation was observed on the surface of most solid substrates. The number of nanoparticles on the cover-slide increased with immersion time, but long periods of immersion (>2 h) resulted in particle

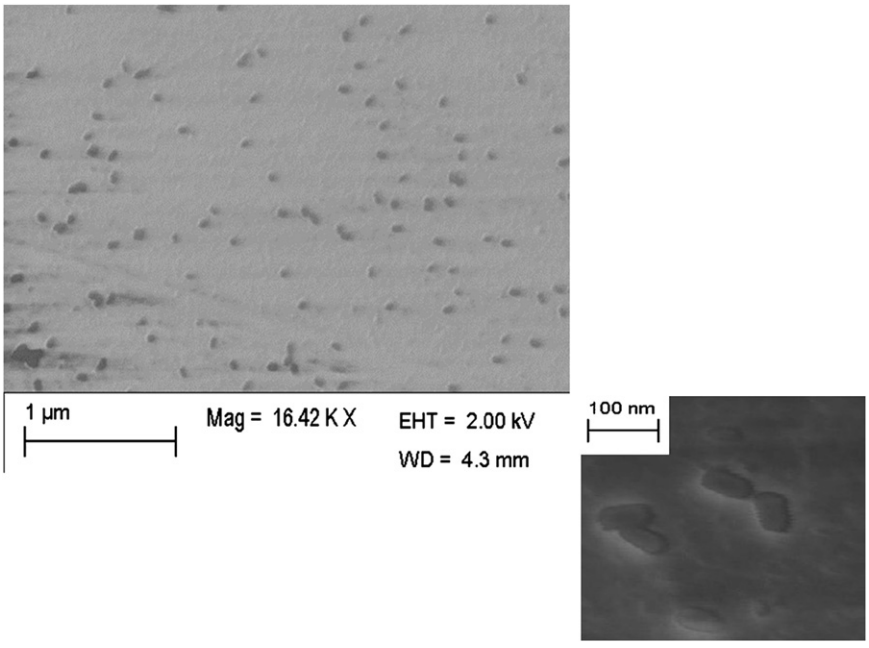

Fig. 1. Scanning electron microscope images of nanorods on the glass coverslide with different magnifications.

aggregation. A bright field illumination image of the resulting surface after ~24 h of immersion is shown in Fig. 2. The aggregation of NRs appears in the absorbance spectrum of the substrate, which shows spectral features at higher wavelengths than the spectrum of dispersed NRs.

The SPR spectra of Au NRs may be altered by two factors: the aspect ratio of the longitudinal to transversal dimensions, and the refractive index of the surrounding medium. The detection of mercury with Au NRs suspended in CTAB aqueous solutions is accomplished because the amalgam formation at the longitudinal ends of the mercury changes the aspect ratio (the aspect ratio approaches unity) as the concentration of mercury increases [18]. Assuming the same type of phenomenon with surface immobilized NRs, the ultimate sensitivity for mercury sensing would probably result from monitoring the SPR of single NRs on the surface of the solid substrate.

3.2. Mercury detection

The NRs response to mercury must be measured in a way that minimizes changes in refractive index while the mercury concentration is measured. To distinguish between changes in the absorbance spectra that result from alterations in the refractive index, and changes in spectra that arise from mercury–Au amalgam formation, absorbance spectra of NRs suspended in solution were recorded and compared to spectra of the NRs chemically immobilized to a silica substrate. The resulting spectra (normalized for ease of comparison) are shown in Fig. 3 for two different samples of NRs with different aspect ratios. When immobilized on the substrate, the absorbance maxima of the LSPR mode exhibit a shift to longer wavelengths. The shift in the spectra can be attributed to a change in the refractive index of the medium surrounding the NRs in contact with the thiol surface. It has been previously reported that increasing the refractive index of the medium surrounding the nanoparticles results in a λ_{max} shift ($\Delta\lambda$) to longer wavelengths; while decreasing the refractive index results in a blue spectral shift [19].

In order to attribute the shifting wavelength response to the presence of mercury rather than the refractive index change resulting from NRs immobilization, the spectra of immobilized gold NRs was recorded prior to mercury addition, and the change in wavelength was monitored with respect to the λ_{max} of the immobilized NRs. Upon addition of the reduced mercury solution, the spectra showed a decrease in the SPR wavelength (Fig. 4A). The change in λ_{max} was plotted as a function of the ratio between the molar concentration of mercury ([Hg]) and the number of NR in solution, yielding a linear calibration curve (Fig. 3B).

It is important to note that the extent to which the aspect ratio of the NRs changes is dependent upon the number of nanoparticles present for a given concentration of mercury. This is an important parameter regardless of whether the mercury is detected with a suspension of NRs or with immobilized NRs. Hence, the calibration for the quantification of mercury depends upon the change in wavelength per NR. The concentration of NRS in solution is commonly determined by measuring the

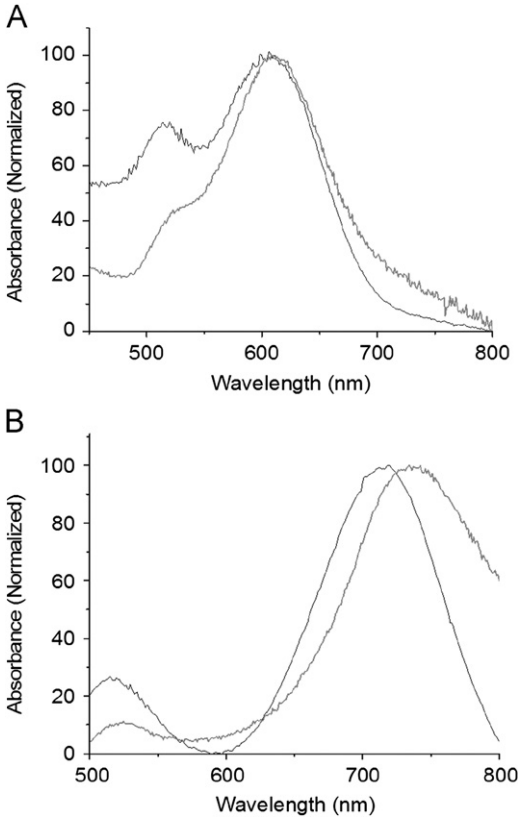

Fig. 3. (A) Absorbance spectra of gold nanorods with dimensions 25 × 51 nm, and (B) nanorods with dimensions 25 × 71 nm. The solid black line represents nanorods suspended in aqueous solution; the gray line is the response of nanorods immobilized on the substrate in aqueous medium, dashed line shows immobilized nanorods in air.

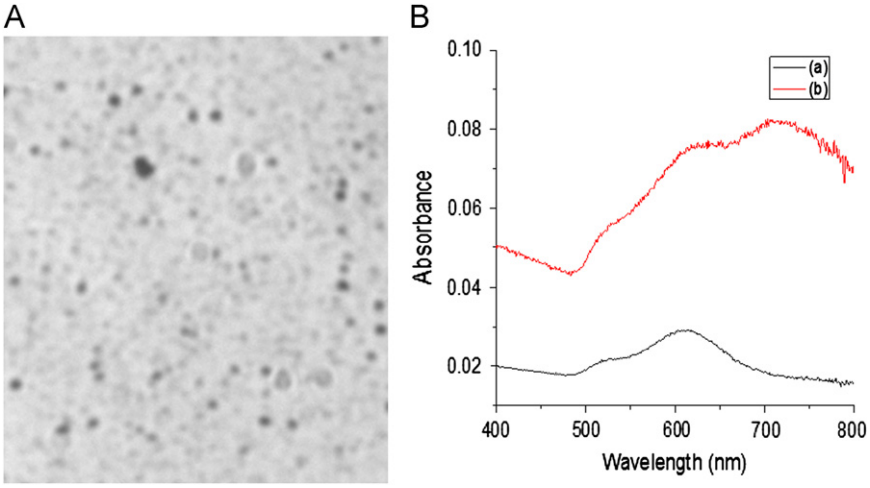

Fig. 2. Images of gold nanorods with longitudinal SPR peak of 615 nm immobilized on glass substrates. (A) Bright field image of gold nanorods with nanorod aggregation. (B) UV/Vis plot of gold nanorods with (a) and without (b) aggregation.

absorbance, which was the technique employed here. The number of NRs immobilized on the substrate was determined by measuring the absorbance spectrum and calculating the concentration of nanoparticles in the solution while the solution concentration was depleted by immobilization onto the glass cover-slide. The absorbance data were baseline corrected and the difference in absorbance used to calculate the number of nanoparticles per unit surface area of the cover-slide Fig. 4.

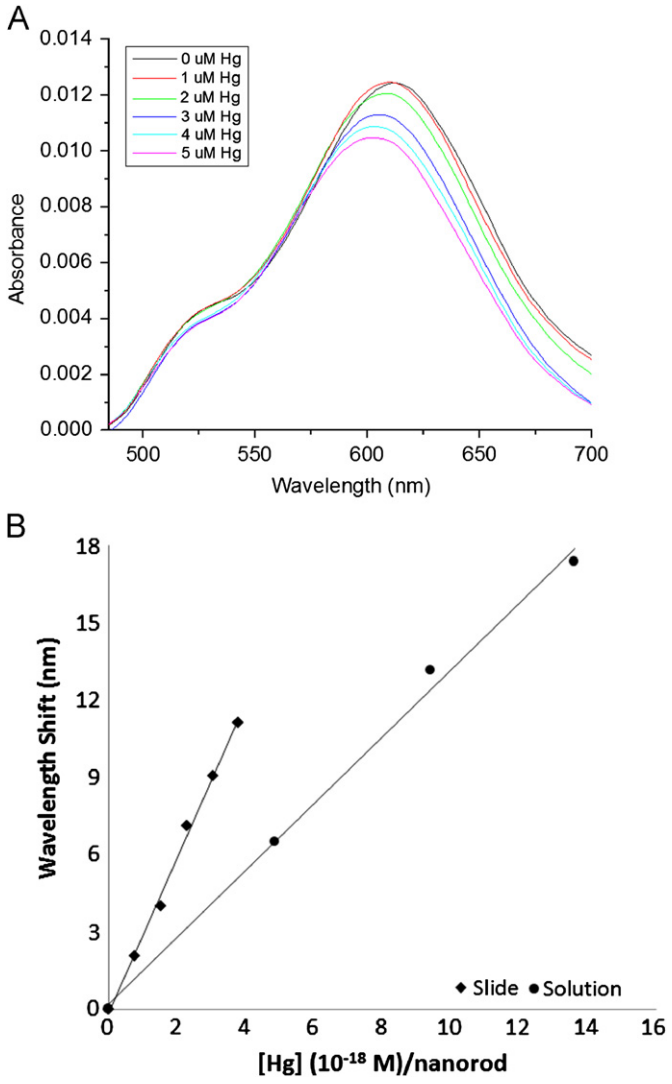

Fig. 4. (A) Absorbance spectra of immobilized gold nanorods in aqueous solution with addition of reduced mercury. (B) Calibration curve showing the change in the SPR response of the sensor in the presence of mercury as well as solution nanoparticles.

3.3. Analytical figures of merit

The AFOM were investigated for two types of sensors, i.e. immobilized Au NRs on solid substrates and Au NRs suspended in liquid solutions. 25×51 nm Au NRs were used in both types of sensors. After estimating the number of particles present on the surface of each sensing device, the SPR response ($\Delta\lambda$) in the presence of mercury was plotted as a function of the ratio between [Hg] and the number of NR on the surface of the sensor. Plotting $\Delta\lambda$ as a function of [Hg]/NR eliminates potential sensitivity variations due to differences in nanoparticle density on the surface of the substrate. The obtained results are summarized in Table 1. Each calibration curve was built with a minimum of five mercury concentrations. For each concentration plotted in the calibration graph, $\Delta\lambda$ was the average of three determinations taken from three spectral runs. No efforts were made to obtain the upper limit of the linear concentration range. The linear fittings ($\Delta\lambda = b \cdot [Hg]/NR + a$) and the statistics of the fittings ($a \pm s_a$ and $b \pm s_b$) were calculated with the least squares method and are shown in Table 1 [20]. The correlation coefficients of the calibration curves were close to unity; *F*-value of 5.1 was calculated for solution calibration (the critical *F*-value is 19.1) indicating that the calibration is linear with 95% confidence [20]. The sensitivity ($\Delta\lambda \cdot NR/[Hg]$; units of nm M^{-1}) of the sensing devices was calculated as the slope (b) of the calibration curve. The limits of detection were calculated using the equations recommended by the International Union of Pure and Applied Chemistry.[21]

Comparison of the 25×51 nm NR in solution with the 25×51 nm NR immobilized on solid substrates shows sensitivities of the same order of magnitude. Apparently, the chemical attachment of NR to the surface of the substrate does not affect significantly the surface of Au available for mercury interaction at the tips of the NRs. This is in good agreement with the SEM images that show most Au NR flattened on the surface of the substrate (see Fig. 1). The lower LOD with Au NR immobilized on solid substrates result from their approximately two times ($\sim 2x$) better sensitivity and the $\sim 3x$ smaller standard deviation of the linear intercept. One possibility for the poorer reproducibility of measurements in liquid solutions is the scatter resulting from the longer optical path length and the random motions of Au NRs.

3.4. Interference studies with the solid substrate Au NR sensor

The utility of a mercury sensor relies upon its sensitivity for mercury without interference by other species, in this case inorganic ions that could be present, and reduced with the $NaBH_4$ along with the mercury, in a sample matrix. Our selection of potential interferences followed the Environmental Protection

Table 1
Analytical figures of merit for mercury detection using gold nanorods.

$\Delta\lambda = b \cdot [Hg]/NR + a$[1]	Solution with 25×51 nm NR $\Delta\lambda = 1.30 \times 10^{18} \cdot [Hg]/NR + 0.2$	Solid substrate with 25×51 nm NR $\Delta\lambda = 2.99 \times 10^{18} \cdot [Hg]/NR - 0.1$
Correlation coefficient	0.9952	0.9957
Sensitivity ($\Delta\lambda \cdot NR \cdot [Hg]$)[2]	1.30×10^{18} nm NR M^{-1}	2.99×10^{18} nm NR M^{-1}
Standard deviation of the slope[3]	$\pm 0.06 \times 10^{18}$ nm NR M^{-1}	$\pm 0.09 \times 10^{18}$ nm NR M^{-1}
Standard deviation of the intercept[3]	± 0.6 nm	± 0.2 nm
LOD (M/NR)[4]	2.49×10^{-18}	3.24×10^{-19}

[1] Equation for best linear fit; *b*=slope; *a*=intercept.
[2] Sensitivity=slope of calibration curve.
[3] Calculated according to Ref. 20.
[4] LOD=Limit of detection. Calculated according to Ref. 21.

Table 2
Shift in absorbance maximum wavelength for gold nanorod sensor in the presence of 5 μM of the listed potentially interfering species.

Compound	$\Delta\lambda_{max}$ (nm)
As_2O_5	0.5 ± 0.1
$Ba(C_2H_3O_2)_2$	-0.5 ± 0.1
$CuSO_4$	-0.5 ± 0.1
NaCl	0.0 ± 0.3
$Pb(NO_3)_2$	-0.7 ± 0.1

Agency list of soluble inorganic ions (arsenic, barium, copper, sodium and lead) and a variety of counterions (oxide, acetate, sulfate, chloride and nitrate) commonly found in tap water composition [22]. Each ion was individually tested at the 5.0 μM concentration, i.e. a much higher concentration than the maximum ion concentration allowed by the EPA in tap water samples. The reference signal (λ_{max} of the LSPR of immobilized Au NR) was measured from a solid substrate immersed in Nanopure water prior and after spiking the reference sample with a Nanopure water solution of appropriate ion concentration. The obtained results are summarized in Table 2. Because the standard deviations of the average λ_{max} values are within the experimental error of the reference signal (P=95%; N=3), it is safe to state that none of the ions caused significant spectral shifts that could interfere with the accuracy of mercury detection.

3.5. Quantification of mercury in tap water

The ability of Au NR substrate to detect mercury in tap water was evaluated by standard addition of an unspiked tap water sample. The Au NR substrate was immersed in a cuvette containing 2.0% (volume percent) tap water (reduced with 0.1 M $NaBH_4$). Aliquots (5 μL) of 200.0 μM $HgCl_2$ were added to the cuvette to construct a standard addition curve. The concentration of mercury in tap water would be calculated by extrapolating to the x-intercept of the standard addition curve (Fig. 5A) yielding a concentration of mercury 9.5×10^{-10} M, a value that is actually below the limit of detection for the sensor.

The quantification capabilities for mercury in contaminated tap water were also evaluated by creating a synthetic sample including several of the EPA contaminants previously discussed (in that case, no mercury was present). This test of a synthetic sample would reveal whether the mercury interaction with the potentially interfering species would result in erroneous quantification of the analyte. The synthetic mixture contained all of the following species at their EPA limits (included parenthesis): sodium chloride (7.0×10^{-3} M), copper sulfate (2.1×10^{-5} M), barium acetate (1.5×10^{-5} M), and arsenic (V) oxide (1.3×10^{-7} M), (lead nitrate (7.2×10^{-8} M). The mixture also contained mercury, spiked to a concentration of 2.5×10^{-7} M. The standard addition curve for the analysis is shown in Fig. 5B. The concentration determined from the standard addition plot was $5.0 (\pm 1.6) \times 10^{-7}$ M, which was t-tested and found to be indistinguishable (95% confidence) from the spiked concentration, since $x(\pm ts_x n^{-1/2})$ was $5.0(\pm 4.3) \times 10^{-7}$.

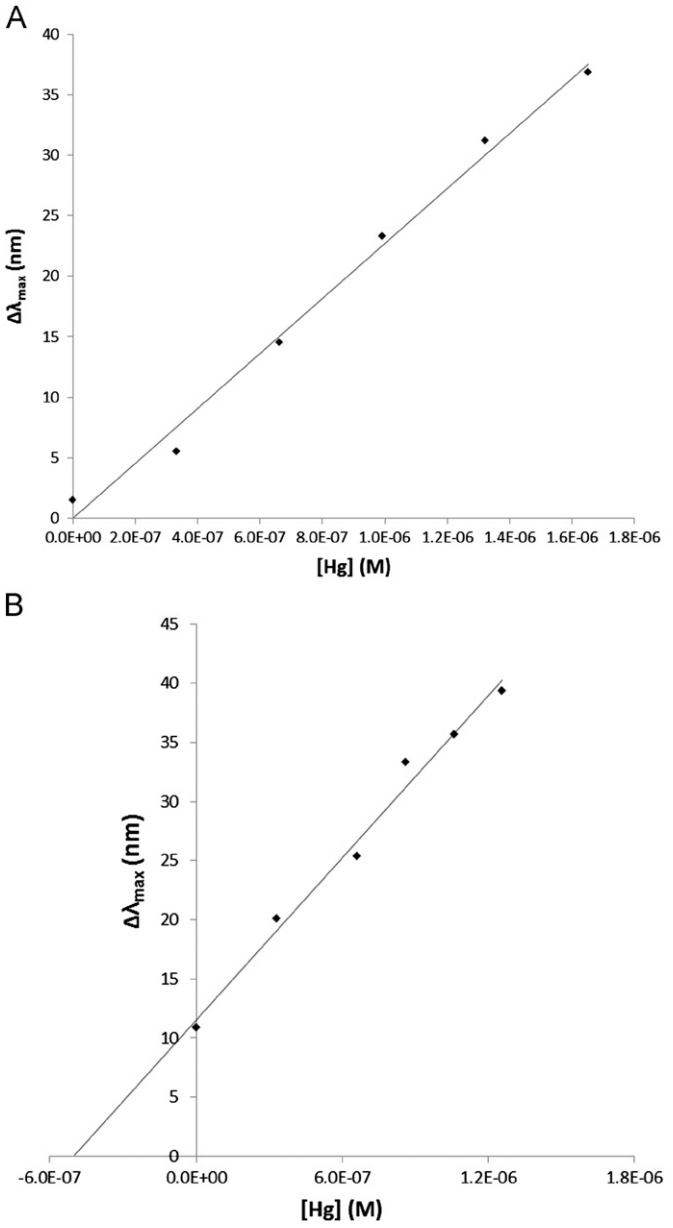

Fig. 5. (A) Standard addition curve for the quantification of mercury in tap water. (B) Standard addition curve for the quantification of a synthetic contaminated water sample containing potentially interfering species.

4. Conclusion

This article details the analytical capabilities of Au NR immobilized on a glass substrate for sensing mercury in water samples. In comparison to solution measurements, the immobilization of Au NR on a solid substrate improves both the sensitivity and the LOD. No interference was observed from several inorganic ions commonly present in tap water samples. This selectivity results from the amalgamation of mercury to Au. The possibility to using glass substrates with immobilized Au NRs is a significant step towards the analysis of mercury in water flows, an approach under current investigation in our lab. By immobilizing Au NRs on the surface of a glass surface it is also possible to examine single NRs via dark field microscopy. Monitoring the spectral shift of the LSPR from a single NR should provide the ultimate sensitivity towards the analysis of mercury with Au NR.

Acknowledgments

We appreciate the assistance of Kirk Scammon in SEM training and support for SEM image acquisition at the Materials Characterization Facility at the University of Central Florida. This work was funded by U.S. Department of Energy (DE-SC0004813).

References

[1] K.M. Mayer, S. Lee, H. Liao, B.C. Rostro, A. Fuentes, P.T. Scully, C.L. Nehl, J.H. Hafner, ACS Nano 2 (2008) 687.
[2] G.J. Nusz, S.M. Marinakos, A.C. Curry, A. Dahlin, F. Hook, A. Wax, A. Chilkoti, Anal. Chem. 80 (2008) 984.
[3] G. Wang, W. Sun, Y. Luo, N. Fang, J. Am. Chem. Soc. 132 (2010) 16417.
[4] J.W. Ha, W. Sun, G. Wang, N. Fang, Chem. Commun. 47 (2011) 7743.
[5] T. Ming, L. Zhao, H. Chen, L. Sun, J. Wang, C. Yan, Nano Lett. 9 (2009) 3896.
[6] W. Ni, Z. Yang, H. Chen, L. Li, J. Wang, J. Am. Chem. Soc. (130) (2008) 6692.
[7] R.A. Alvarez-Puebla, A. Agarwal, P. Manna, B.P. Khanal, P. Aldeanueva-Potl, E. Carbo-Argibay, N. Pazos-Perez, L. Vigderman, E.R. Zubarev, N.A. Kotov, L.M. Liz-Marzan, PNAS 108 (2011) 8157.
[8] K.M. Mayer, J.H. Hafner, Chem. Rev. 111 (2011) 3828.
[9] O. Seitz, M.M. Chehimi, E. Cabet-Deliry, S. Truong, N. Felidj, C. Perruchot, S.J. Greaves, J.F. Watts, Colloids Surf. A: Physicochem., Eng. Aspects 218 (2003) 225.
[10] T. Okamoto, I. Yamaguchi, Opt. Lett. *25* (2000) 372.
[11] K.C. Grabar, R.G. Freeman, M.B. Hommer, M.J. Natan, Anal. Chem. 67 (1995) 735.
[12] E.E.L. Chan, L. Yu, Langmuir 18 (2002) 311.
[13] K.C. Grabar, K.R. Brown, C.D. Keating, S.J. Stranick, S.-L. Tang, M.J. Natan, Anal. Chem. 69 (1997) 471.
[14] E. Kopsyc, K. Pyrzynska, S. Garbos, E. Bulska, Anal. Sci. 16 (2000) 1309.
[15] L. Yu, X. Yan, At. Spectrom. 25 (2004) 145.
[16] Y. Bonfil, M. Brand, E. Kirowa-Eisner, Anal. Chim. Acta 424 (2000) 65.
[17] B. Palenzuela, L. Manganiello, A. Riso, M. Valcarcel, Anal. Chim. Acta 511 (2004) 289.
[18] M. Rex, F.E. Hernandez, A.D. Campiglia, Anal. Chem. *78* (2006) 445.
[19] S. Link, B. Mohamed, M.A. El-Sayed, J. Phys. Chem. B 103 (1999) 3073.
[20] K. Danzer, L.A. Currie, Pure & Appl. Chem. 70 (1998) 993.
[21] L.A. Currie, Pure & Appl. Chem. 67 (1995) 1699.
[22] 〈http://www.epa.gov/safewater/consumer/pdf/mcl.pdf〉.